

Probing electron-dominated current sheets in the collisionless turbulent solar wind by determining the electron-to-ion bulk speed ratio

JÖRG BÜCHNER,^{1,2} NEERAJ JAIN,² OLGA KHABAROVA,³ TIMOTHY SAGITOV,³
HELMI MALOVA,^{4,5} AND ROMAN KISLOV⁴

¹*Max Planck Institute for Solar System Research, 37077 Göttingen, Germany*

²*Center for Astronomy and Astrophysics, Technical University of Berlin, 10623 Berlin, Germany*

³*Pushkov Institute of Terrestrial Magnetism, Ionosphere and Radio Wave Propagation of the Russian Academy of Sciences (IZMIRAN), 108840 Moscow, Russia;*

⁴*Space Research Institute of the Russian Academy of Sciences (IKIRAN), 117997 Moscow, Russia*

⁵*Scobeltsyn Nuclear Physics Institute (NPI), Lomonosov State University, 119991 Moscow, Russia; hmalova@yandex.ru*

ABSTRACT

Current sheets (CSs) are preferred sites of magnetic reconnection and energy dissipation in turbulent collisionless astrophysical plasmas. In our prior theoretical studies of processes associated with the CS formation in turbulent plasmas, for which we utilized fully kinetic and hybrid code simulations with ions considered as particles and electrons - as a massless fluid (Jain et al. 2021), we found that (i) inside ion-scale CSs thin electron-scale CSs form (Azizabadi et al. 2021), (ii) with the CS thinning the electron-to-ion bulk speed ratio u_e/u_i increases, and (iii) the electrons become the main carriers of the electric currents and contributors to energy dissipation. The question arises: is it possible to find electron-dominated-CSs in natural plasmas, using the u_e/u_i signature as a search criterion? We apply this parameter to the solar wind to locate electron CSs there at least approximately. Existing methods of identification CSs in the solar wind focus on the search for ion-scale structures by considering changes in the magnetic field and plasma parameters (Khabarova et al. 2021). We now found that electron-dominated CSs observed during a period of quiet solar wind conditions at 1 AU can be identified by sharp variations of u_e/u_i often localized in the vicinity of ion-scale CSs, showing the same clustering. We conclude that u_e/u_i may be used as one of key parameters for probing CSs and the role of electrons in them.

Keywords: Current sheets, kinetic plasma turbulence, hybrid simulations, solar wind

1. INTRODUCTION

Spacecraft routinely observe the electric-current-carrying thin plasma layers, current sheets (CSs), in collisionless space plasmas (e.g., (Nakamura et al. 2006; Greco et al. 2009; Jain et al. 2021; Azizabadi et al. 2021; Sundkvist et al. 2007; Podesta 2017; Khabarova et al. 2021)). In the solar wind, CSs are formed at discontinuities that separate regions with differently directed magnetic fields (Syrovatskiĭ 1971). Such discontinuities may represent a continuation of large-scale neutral lines of the solar origin as well as form at edges of various streams and flows, between magnetic islands and result from magnetic reconnection, instabilities and wave propagation (Khabarova et al. 2021). CS structures are known to play a significant role in the development of turbulence and energy release in a form of heating or particle acceleration (Muñoz et al. 2014; Khabarova et al. 2015, 2016; Muñoz & Büchner 2018a; Jain et al. 2021; Lazarian et al. 2020; Azizabadi et al. 2021; Khabarova et al. 2021; Pezzi et al. 2021). They can contribute to an energy cascade when their magnetic energy is transported from larger to shorter scales until it is transferred to the kinetic energy of particles via magnetic reconnection and/or dissipation.

In collisionless plasmas, CSs may thin down to kinetic plasma scales, such as the inertial length or gyro-radii of particles, whichever is reached earlier (Jain et al. 2021; Azizabadi et al. 2021). Then kinetic instabilities would cause additional, small scale turbulence which directly dissipates energy or allows fast magnetic reconnection. This sequence of events is well-known for large, long-lived current sheets of the solar origin, such as the heliospheric current sheet (HCS) that creates a wide cloud of secondary, smaller-scale CSs and other dynamically evolving coherent structures in its vicinity (see (Khabarova et al. 2021) and references therein). The specific of dissipation mechanisms, a threshold of micro-instabilities and an efficiency of the energy conversion depend on the structure and properties of CSs, in particular, on the kind of particles carrying the electric current, their possible anisotropic distribution and other macro- and microscopic plasma parameters.

On the other hand, turbulence can create thin and short-lived CSs (e.g., (Howes 2016) which are found to occur ubiquitously in numerical simulations of dynamical processes in space turbulent plasmas (Maron & Goldreich 2001; Franci et al. 2015; Perri et al. 2012; Howes 2016). In the solar wind, this scenario realizes far from long-lived and large-scale CSs, in undisturbed plasma. CSs created by turbulence may merge and form larger and longer-lived structures if plasma is impacted by waves, instabilities or flows.

In order to understand peculiarities of the CS formation, mainly macroscopic, fluid-type numerical simulations have been carried out (see, e.g. (Biskamp & Welter 1989; Bárta et al. 2010; Bárta et al. 2011)). Based on the results of restricted electron-MHD simulations, it has been suggested that the CSs with a thicknesses ranging down to electron scales are responsible for structuring 3D reconnection (Jain & Büchner 2014a,b). Both observational studies and numerical simulations suggest that a large

fraction of the total magnetic energy is dissipated in and around kinetic-scale-CSs that form self-consistently and possess a significant power of turbulence (Matthaeus et al. 2015; Borovsky 2010).

The occurrence of CSs is known to determine the shape of the power spectrum of magnetic field variations in the solar wind. This interesting fact has been discovered by Gang Li in 2011 (Li et al. 2011) and then recently confirmed by Borovsky and Burkholder (Borovsky & Burkholder 2020). Gang Li showed that the current-sheet-abundant solar wind is characterized by the Kolmogorov-like power spectrum with the slope of -1.7, and the solar wind without current sheets demonstrates Iroshnikov-Kraichnan scaling with a slope of -1.5. Borovsky and Burkholder (Borovsky & Burkholder 2020) performed an analysis of factors forming a shape of the spectrum and concluded that both purely topological characteristics of CSs and dynamical processes occurring at them and their vicinity impact the spectrum considerably.

Since a dissipation mechanism in and around CSs is not quite clear yet, their visual or automated identification in space and subsequent thorough studies of their properties are crucial to understand numerous processes associated with these plasma objects. Spacecraft investigations of the last two decades combined with theoretical expectations revealed a unique structure of current layers in space plasma that can consist of an extremely thin electron current embedded in a thicker ion/proton current sheet. In turn, this configuration can often be embedded in a wider plasma sheet with a rather weak background CS current sheet. Satellite observations in the Earth's magnetosphere, spacecraft observations in the solar wind and theoretical investigations allowed understanding of general properties of proton-current-dominated CSs with a width up to several proton gyroradii. As for electron, thinner currents, prior limitations of thin CS models and insufficiency of spatial/temporal resolution of observations gave only rough estimates of the thickness and the amplitude of the electron current peak (see (Zelenyi et al. 2004, 2011, 2019; Malova et al. 2012, 2013, 2017) and references therein).

An appearance of modern instruments with a high resolution for the magnetic field have provided researchers an opportunity to investigate a new kind of CSs called super thin CS current sheets (STCSs) observed in the course of new spacecraft missions such as MAVEN in the Martian magnetotail (Grigorenko et al. 2019). A half-thickness of the STCSs is about a few or less electron gyroradii, therefore, these current layers can be considered as electron-dominated CSs. The Magnetospheric Multiscale (MMS) mission with its electron-scale tetrahedron configuration has also been very useful in understanding properties of electron-scale STCSs in both the Earth's magnetopause and the magnetotail (e.g., (Phan et al. 2016; Dong et al. 2018)).

Meanwhile, an identification of such extra-thin current layers in the solar wind is still complicated because of the insufficiently of the resolution of the magnetic field measurements and the necessity of multi-scale missions owing to which thin CSs were

discovered and studied in the terrestrial magnetotail (Sergeev et al. 1993; Runov et al. 2003; Runov et al. 2006).

Note that various criteria are used for an identification of proton-dominated-CSs. Most commonly, significant rotation of the magnetic field vector (sometimes, from one direction to the opposite) and signatures of the crossing of a neutral line are employed to distinguish between ordinary discontinuities and CSs. These are primary signs of CS crossings. Additionally, observers analyze the behavior of plasma parameters, namely, the plasma beta (β) that sharply increases at strong CSs and the ratio of the Alfvén speed to the solar wind speed (that usually decreases at CSs). The latter are secondary signatures identifying CSs. An overview of both visual and automated methods of CS identification in the heliosphere can be found in (Khabarova et al. 2021).

Since correct measurements of electron currents are impossible for most spacecraft operating in the solar wind and having a resolution of one-three seconds for the magnetic field (e.g., (Kellogg et al. 2003, 2006)), it would be interesting and useful to find secondary or indirect signatures of electron-dominated CSs. Theoretical studies and numerical simulations may help. A theoretical approach in a frame of a hybrid 1D or 2D models in which ions are considered with a quasi-adiabatic approach and the electron motion is treated as an MHD flow is known to be the most perspective in the description of such thin multilayered CSs (Zelenyi et al. 2004, 2011; Petrukovich et al. 2011; Malova et al. 2012, 2013). A pioneering work (Zelenyi et al. 2020) has provided the basis of the theory of super-thin current layers, and recent numerical simulations allowed finding the way to identify electron-dominated CSs via an analysis of spatial variations of plasma parameters (Jain et al. 2021; Azizabadi et al. 2021).

For a better understanding of the CS formation and their expected thinning down to kinetic scales different kinds of numerical simulations have been carried utilizing a variety of different plasma models like, e.g., hybrid codes which consider ions as particles and electrons as a fluid (Jain et al. 2021; Azizabadi et al. 2021). The latter investigation revealed, supported by theoretical estimates, an extra-criterion which can be used for a better understanding of the structure of CSs in turbulent plasmas. This criterion is based on the finding that within thinning CSs the (shear) flow velocity of the current carrying electrons in the direction parallel to the ambient magnetic field ($|u_e|$) should significantly exceed by large the ion bulk flow velocity ($|u_i|$) in this direction. At the same time the plasma density would vary only weakly (less than 10%) throughout the CSs. Thus, the ratio of electron over the ion bulk flow velocities ($|u_e/u_i|$) should become very large. We first describe this jump criterium of $|u_e/u_i|$ within CSs and then search for sharp variations of the parameter in the turbulent solar wind plasma utilizing the WIND spacecraft observations.

A supporting observational case study that follows the theoretical part is aimed at a preliminary estimation of the ability of the u_e/u_i parameter to recognize plasma structures that may be associated with electron-dominated CSs. We also raise impor-

tant questions regarding the relation between electron- and ion-dominated CSs. Do they always spatially coincide in the solar wind? Can we observe electron-dominated CSs exist independently of ion-dominated CSs?

The structure of the manuscript is as follows. First, in section 2, we describe the simulation approach and its results revealing a jump criterion for $|u_e/u_i|$ - (or $|u_e/u_i|$). In section 3 we theoretically estimate the value of $|u_e/u_i|$ in thinning current sheets. In section 4 we describe the utilized WIND spacecraft observations aimed at identifying plasma structures that may be associated with strong electron-dominated CSs. The results of theour data analysis are provided in section 5. The conclusions of our investigation are drawn and discussed in section 6.

2. SIMULATION RESULTS

We carried out hybrid code simulations of a turbulent plasma in which we treated ions as particles and electrons as an inertia-less fluid on a two-dimensional mesh spanning over an x-y plane. For this sake we utilized the PIC-hybrid code A.I.K.E.F. (Müller et al. 2011). We initialized the simulations with random-phased fluctuating magnetic fields and plasma velocities within a wave number range $|k_{x,y}d_i| < 0.2$ ($k_{x,y} \neq 0$). Here k_x and k_y are wave numbers in the x- and y-directions, respectively, $d_i = v_{Ai}/\omega_{ci}$, $v_{Ai} = B_0/\sqrt{\mu_0 n_0 m_i}$ and $\omega_{ci} = eB_0/m_i$ are inertial length, Alfvén velocity and cyclotron frequency of ions, respectively (μ_0 is the vacuum magnetic permeability, e the electron charge and m_i the proton mass). The fluctuations are imposed on an isotropic background plasma of uniform density n_0 . All initialized modes have the same energy and a root-mean-square value $B_{rms}/B_0 = 0.24$, where B_0 is the uniform magnetic field applied perpendicular to the simulation plane. Electron and ion plasma beta are $\beta_e = 2\mu_0 n_0 k_B T_e / B_0^2 = 0.5$ and $\beta_i = 2\mu_0 n_0 k_B T_i / B_0^2 = 0.5$, with T_e and T_i being the electron and ion temperatures, respectively and k_B the Boltzmann constant. The simulation box size $256d_i \times 256d_i$ is resolved by 512×512 grid points with 500 macro-particles per cell. The time step was chosen to be $\Delta t = 0.01 \omega_{ci}^{-1}$. Periodic boundary conditions are applied in all directions.

In the course of the evolutions of the initially long-wavelength magnetic and ion velocity fluctuations, current sheets are formed by $\omega_{ci}t = 50$ (Fig. 1). These current sheets later break up developing shorter wavelength turbulence (Daughton et al. 2011; Muñoz & Büchner 2018b; Dahlin et al. 2015), as shown at $\omega_{ci}t = 150$ in Fig. 1. Our hybrid code simulations revealed that within the current sheets the parallel electron bulk flow velocities became much larger than the parallel ion bulk velocities Jain et al. (2021). The perpendicular bulk velocities of electrons and ions, on the other hand, are of the same order but smaller than the parallel bulk velocity of electrons. Therefore net bulk speed of electrons is larger than the net bulk speed of ions.

In space observations, special care has to be taken to distinguish between parallel and perpendicular (to the magnetic field) velocity components. It is typically easier to get net velocity of particles in space observations. In order to interpret the obser-

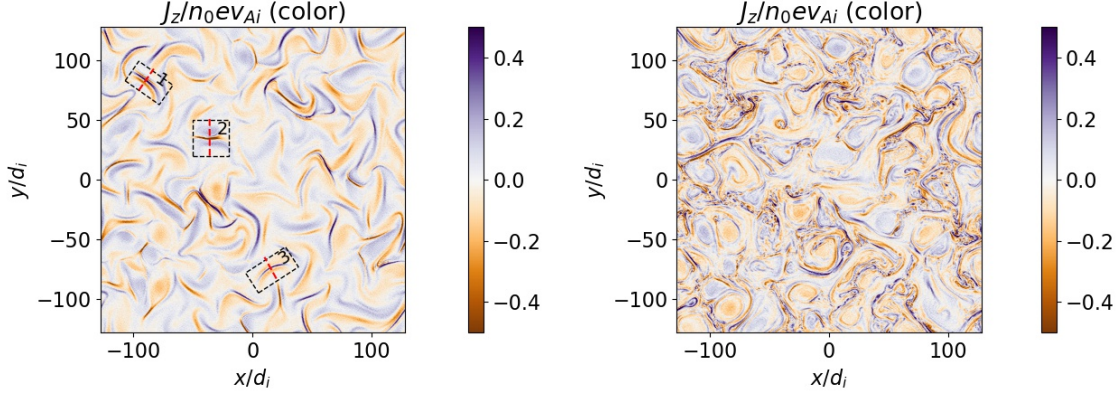


Figure 1. Parallel current density J_z at two moments of time: $\omega_{ci}t = 50$ (left column) and $\omega_{ci}t = 150$ (right column). Three current sheets, numbered 1, 2 and 3, are highlighted at $\omega_{ci}t = 50$ by enclosing them in rectangles with dashed borders. The red line in each rectangle is the current sheet normal.

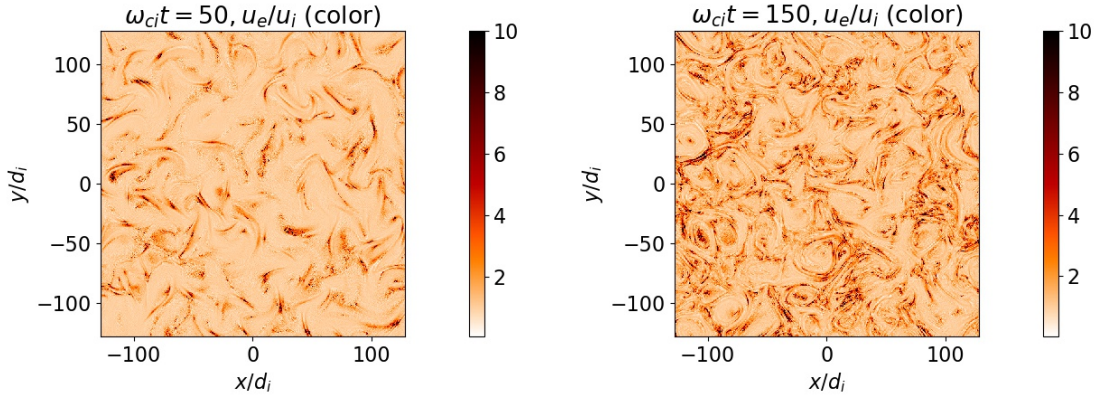


Figure 2. Ratio u_e/u_i of the magnitudes of the electron- ($u_e = |\mathbf{u}_e|$) to the ion-bulk speeds ($u_i = |\mathbf{u}_i|$) at two moments of time: $\omega_{ci}t = 50$ (left column) and $\omega_{ci}t = 150$ (right column).

vations we examined the ratio u_e/u_i of the net bulk velocities $u_e = |\mathbf{u}_e|$ and $u_i = |\mathbf{u}_i|$ of the electrons and ions, respectively. As an example Fig. 2 depicts the iso-lines of $|\mathbf{u}_e|/|\mathbf{u}_i|$ in the simulation plane at $\omega_{ci}t = 50$ and $\omega_{ci}t = 150$. It can be seen that the electron bulk speed u_e exceeds the ion bulk speed u_i by several times in ion-scale current sheets. Moreover, the ratio u_e/u_i enhances as the turbulence evolves from $\omega_{ci}t = 50$ to 150.

In order to detect a jump in u_e/u_i in time series measurements by spacecraft, it is more practical to look at the derivative of u_e/u_i . Figure 3 shows the magnitude of the spatial gradient of u_e/u_i in the simulation plane. It is clear from Figs. 2 and 3 that the value of $|\nabla(u_e/u_i)|$ in CSs is better distinguished from its value outside current sheets as compared to the values of u_e/u_i .

Fig. 4 shows the line-outs of u_e/u_i , $|\nabla(u_e/u_i)|$ and J_z along the normal of the three current sheets (CS-1, CS-2 and CS-3) highlighted in Fig. 1. It can be seen that u_e/u_i takes a jump from its value of the order of unity outside current sheets to at least

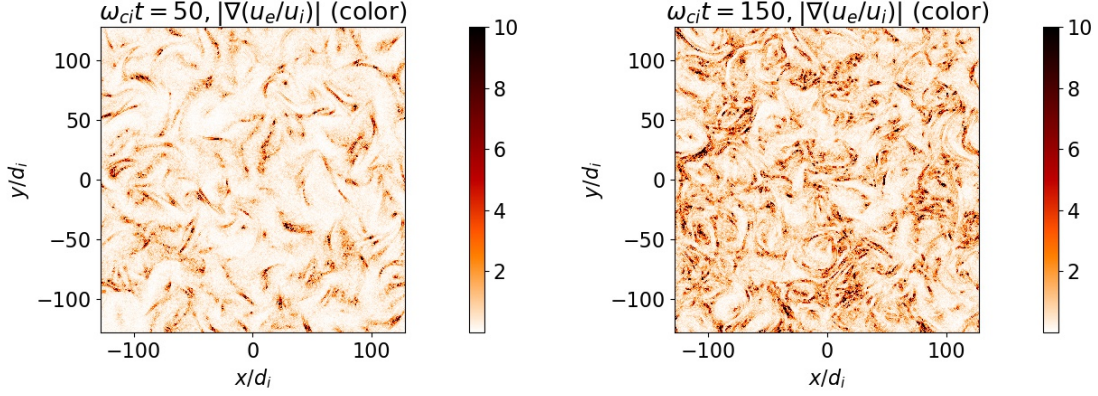


Figure 3. Magnitude of the gradient of the ratio u_e/u_i at two moments of time: $\omega_{ci}t = 50$ (left column) and $\omega_{ci}t = 150$ (right column).

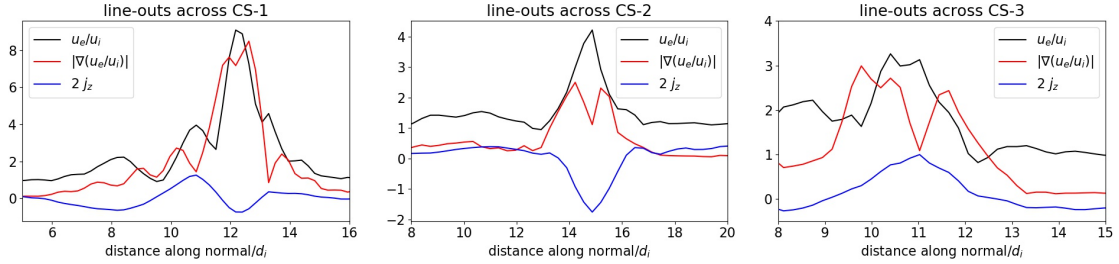


Figure 4. Line-outs of u_e/u_i , $\nabla(u_e/u_i)$ and j_z across the three current sheets (CS-1, CS-2, CS-3) highlighted in Fig. 1 at $\omega_{ci}t = 50$.

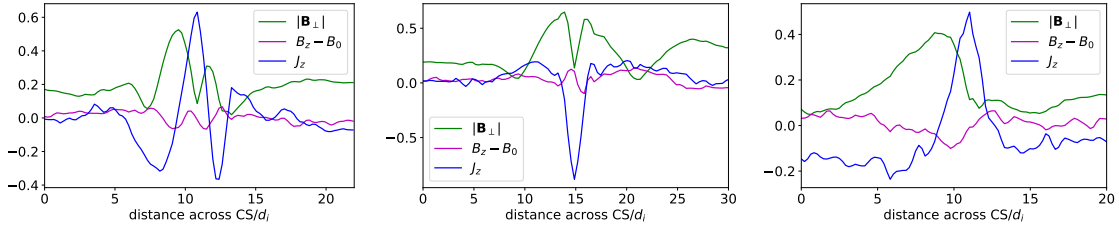


Figure 5. Line-outs of $|B_{\perp}|/B_0$, $(B_z - B_0)/B_0$ and $j_z/(n_0 e v_{Ai})$ across the three current sheets (from left to right: CS-1, CS-2, CS-3) highlighted in Fig. 1 at $\omega_{ci}t = 50$.

several times larger value in CSs. Note that the value of u_e/u_i inside CSs sheets is not unique. It might be different for different CSs. Therefore the actual value of u_e/u_i inside CSs is not as important as the jump in its value from outside to inside the sheets as far as the CS detection is concerned. This jump is characterized by $|\nabla(u_e/u_i)|$. Note that $\nabla(u_e/u_i)$ inside CSs is dominated by the gradient along the current sheet normal which changes sign across the current sheet. A dip in the value of $|\nabla(u_e/u_i)|$ at the peak of u_e/u_i in Fig. 3 corresponds to this change of sign of $\nabla(u_e/u_i)$.

3. THEORETICAL ESTIMATE OF THE RATIO $|U_E/U_I|$

For a quantitative comparison with observations it is appropriate to estimate the expected values of electron and ion bulk flow velocities. Theoretical estimates for the ratio of the out-of-plane electron and ion bulk velocities, $|u_{ez}|/|u_{iz}|$, was obtained approximating ion response as un-magnetized Jain et al. (2021). Here we estimate theoretically the ratio of the total electron and ion bulk velocities, u_e/u_i under the approximation of un-magnetized ions.

For current sheets with thicknesses of the order of ion gyro-radius $\rho_i = \sqrt{\beta}d_i$, ions can be approximated as un-magnetized while electrons are still tied to the magnetic field lines. Fig. 5 shows lineouts across current sheets CS1-CS3 of the turbulent magnetic field components perpendicular ($|\mathbf{B}_\perp|$) and parallel ($B_z - B_0$) to the applied magnetic field $B_0\hat{z}$. The turbulent magnetic field near the current sheet center, where current density peaks, is an order of magnitude smaller than the applied magnetic field ($|\mathbf{B}_\perp|/B_0 \sim (B_z - B_0)/B_0 \sim 0.1$). Therefore, we take parallel and perpendicular directions inside current sheets (approximately) with respect to the applied magnetic field $\mathbf{B}_0 = B_0\hat{z}$. We can then obtain ion bulk velocity \mathbf{u}_i from ion's momentum equation neglecting Lorentz force, perpendicular electron bulk velocity $\mathbf{u}_{e\perp}$ as $E \times B$ drift from Ohm's law and parallel electron bulk velocity \mathbf{u}_{ez} from Ampere's law.

$$\frac{\partial \mathbf{u}_i}{\partial t} = \frac{e\mathbf{E}}{m_i} \quad (1)$$

$$\mathbf{u}_{e\perp} = \frac{\mathbf{E}_\perp \times \mathbf{B}}{B^2} \quad (2)$$

$$\mathbf{u}_{ez} = \mathbf{u}_{iz} - \frac{\nabla_\perp \times \mathbf{B}_\perp}{\mu_0 n e} \quad (3)$$

Electric and magnetic fields are related by Faraday's law.

$$\nabla_\perp \times \mathbf{E} = -\frac{\partial \mathbf{B}}{\partial t} \quad (4)$$

Here $\nabla_\perp \equiv \hat{x}\partial/\partial x + \hat{y}\partial/\partial y$. In Eq. 1, the convective derivative $(\mathbf{u}_i \cdot \nabla)\mathbf{u}_i$ is neglected compared to the time derivative inside current sheets under the approximation $|(\mathbf{u}_i \cdot \nabla)\mathbf{u}_i|/|\partial \mathbf{u}_i/\partial t| \sim u_{i,\perp}/v_{Ai} \sim 0.1 \ll 1$ (for $\partial/\partial t \sim v_{Ai}/L$ and $\nabla_\perp \sim L^{-1}$) as it was demonstrated by simulations Jain et al. (2021). Eqs. 1 and 2 give estimates as $u_{i\perp} \sim LE_\perp/d_i B$, $u_{iz} \sim LE_z/d_i B$ and $u_{e\perp} \sim E_\perp B_z/B^2$.

Estimating $E_\perp \sim b_z v_{Ai}$ and $E_z \sim b_\perp v_{Ai}$ from Faraday's law, we get,

$$u_{i\perp} \sim v_{Ai} L b_z / d_i B \quad (5)$$

$$u_{iz} \sim v_{Ai} L b_\perp / d_i B \quad (6)$$

$$u_{e\perp} \sim v_{Ai} b_z B_z / B^2 \quad (7)$$

Here $b_\perp = |\mathbf{B}_\perp|$ and $b_z = B_z - B_0$ are turbulent magnetic field components. The first term ($|u_{iz}| \sim v_{Ai} L b_\perp / d_i B$) on the RHS of Eq. 3 can be neglected in comparison to the second term ($|\nabla_\perp \times \mathbf{B}_\perp|/\mu_0 n e \sim v_{Ai} d_i b_\perp / LB$) for perpendicular spatial scale

lengths $L \ll d_i$ giving,

$$u_{ez} \sim v_{Ai} d_i b_{\perp} / LB. \quad (8)$$

The parallel and perpendicular components of electron and ion bulk velocities can now be compared inside current sheets using Eqs. (5)-(8). From Eqs. (5) and (7), $u_{e\perp}/u_{i\perp} \sim (B_z/B)(d_i/L)$. For un-magnetized ions ($L < \rho_i \sim d_i$) and $B_z \sim B \sim B_0$, $u_{e\perp}/u_{i\perp} \sim d_i/L > 1$ consistent with the results of the hybrid simulations [Jain et al. \(2021\)](#). Inside current sheets, the perpendicular ion bulk velocity is typically smaller than the perpendicular electron bulk velocity due to the demagnetization of ions. From Eqs. (6) and (8), $u_{ez}/u_{iz} \sim d_i^2/L^2 > 1$. Note that both the ratios $u_{e\perp}/u_{i\perp}$ and u_{ez}/u_{iz} are greater than unity but $u_{ez}/u_{iz} > u_{e\perp}/u_{i\perp}$ consistent with the simulations [Jain et al. \(2021\)](#). Using $B_z \sim B$, $b_{\perp} \sim b_z$ and $d_i^2/L^2 \gg 1$, the ratio of the net electron and ion bulk velocities, $u_e = (u_{e\perp}^2 + u_{ez}^2)^{1/2}$ and $u_i = (u_{i\perp}^2 + u_{iz}^2)^{1/2}$ respectively, can be written as,

$$\frac{u_e}{u_i} \sim \frac{d_i^2}{L^2} \frac{b_{\perp}}{(b_{\perp}^2 + b_z^2)^{1/2}}. \quad (9)$$

The ratio u_e/u_i is smaller than the ratio u_{ez}/u_{iz} by a factor of the order of unity, again consistent with the results of the hybrid simulations [Jain et al. \(2021\)](#). With the CS thinning, therefore, the current in the sheet is confirmed to be increasingly carried by the electrons.

4. OBSERVATIONS

Proton-scale CSs in the solar wind are usually identified using the magnetic field and plasma data from spacecraft. Methods that allow an automated recognition of such CSs have recently been developed, helping understanding statistical properties of ion-dominated CSs observed under different conditions in the solar wind plasma (see [Khabarova et al. 2021](#)) and references therein).

As noted in the Introduction, in most cases one cannot directly observe electron-scale current sheets in the solar wind, first of all, because of the absence of the constellation-type spacecraft operating there. The point is that a correct calculation of the electric current density suggests carrying out simultaneous measurements of plasma and magnetic field parameters at several rather close points. Nowadays, only the MMS and Cluster magnetospheric missions can be used for such a purpose, but the problem is that periods when their path lays in the solar wind, upstream the terrestrial bow shock, are very short.

In the case of single spacecraft measurements, the electric current density can only be estimated roughly. This is the reason why finding the location of CSs in the solar wind is always a matter of the analysis of several parameters that specifically vary at CS crossings (as shown in [Khabarova et al. 2021](#); [Khabarova et al. 2021](#)).

The second problem is that a resolution of measurements of the magnetic field in the solar wind is usually about one second that corresponds to one-two proton gyroradii.

This is satisfactory for identifying ordinary ion-scale CSs, but this makes impossible direct observations of much thinner electron-scale CSs that often carry the current larger than that carried by ions (Wang et al. 2018; Podesta 2017).

Meanwhile, it is often useful to know at least an approximate location of CSs determined by electron-carried currents, for example, to see how they are related to ion CSs. We will show that despite the obstacles discussed above, one may consider indirect observational signatures of electron-determined CSs to recognize them from the solar wind data. After simulations have shown that the u_e/u_i ratio may represent an important parameter reflecting the occurrence of electron-dominated scale CSs, we check this using the solar wind data on the electron and proton velocity data at 1 AU from the Wind spacecraft and compare a location of electron-dominated CSs with a location of ion-dominated CS obtained from the method described in (Khabarova et al. 2021). As we show below, sharp variations in the u_e/u_i parameter can potentially point out a strong electron-dominated CS located somewhere within the region crossed by a spacecraft for 3 seconds (which is a typical temporal resolution of the solar wind spacecraft for the magnetic field). We further compare locations of structures presumably representing electron-dominated CSs with those of ion-dominated CSs obtained from the method described in (Khabarova et al. 2021).

Theoretical predictions and observations in the magnetosphere suggest that electron CSs may both be embedded in wider ion-scale CSs and exist separately of them. With a one-three second resolution of observations in the solar wind, this may look as either simultaneous occurrence of ion- and electron-determined CSs at one place or the occurrence of electron CSs without the presence of ion CSs in their vicinity. So far, there have not been studies letting us know if electron CSs can form in the solar wind independently of ion CSs. Comparing the spatial distribution of ion-dominated CSs and electron-dominated CSs identified via independent automated methods cannot answer this question directly but may give us a hint on where electron-dominated CSs may occur.

A preliminary study carried out below answers this question positively.

4.1. *Data and time interval selection*

Solar Wind Experiment (SWE) Electron Data Sources are available at NASA's Space Physics Data Facility (SPDF) HTTPS site <https://cdaweb.gsfc.nasa.gov/index.html>. They allow finding the velocity of electrons (u_e) necessary for the study. We further use the ion (proton) velocity (u_i) obtained by the Wind spacecraft 3-D Plasma and Energetic Particle Investigation experiment (Wind 3DP, <http://sprg.ssl.berkeley.edu/wind3dp>). From those data we calculate the u_e/u_i ratio and find the total magnetic field B .

Additionally, we employ the solar wind key parameters to compile a list of ion current sheets via the automated method that considers sharp variations in the total magnetic field, β , and the Alfvén speed V_a to the solar wind speed V ratio (Khabarova

et al. 2021). This is the basis of the three-parameter method, using which the IZMIRAN database of current sheets has been built (see <https://csdb.izmiran.ru/>). Summarizing, the following Wind data from the SPDF website have been used:

- WI_H2_MFI - Wind Magnetic Fields Investigation, high-resolution definitive data (the interplanetary magnetic field (IMF));
- WI_PM_3DP - Ion moments (the velocity, the density, and the temperature of the solar wind protons);
- WI_EM_3DP - Electron Plasma moments (the electron velocity).

The u_e/u_i data have the three second resolution, and the three key parameters to identify the ion current sheet location via the method described in (Khabarova et al. 2021) are calculated with a one second cadence.

We have selected a very quiet solar wind period from 00:00 February 13, 1998 to 12:00 February 14, 1998 during which the near-Earth plasma was not affected by either interplanetary coronal mass ejections (ICMEs) or stream interaction regions (SIRs).

One can see in the three upper panels of Fig. 6 that the B_y and B_z components of the IMF in the Geocentric Solsolar Ecliptic (GSE) coordinate system vary around zero, and the B_x component shows a slow transition from the negative to positive IMF sector, suggesting a crossing of the heliospheric plasma sheet (HPS). The HPS is a wide area filled with numerous CSs produced, on the one hand, by magnetic reconnection and instabilities developing at the HCS embedded in the HPS, and, on the other hand, by the same processes occurring at other strong and long-lived CSs representing an extension of former streamers expanding from the solar corona (Maiewski et al. 2020). Because of this, the IMF components may vary around zero for hours, and the IMF does not immediately change its direction at the HCS within the HPS (Khabarova et al. 2021).

As seen in the two bottom panels of Fig. 6, the spacecraft is in the slow solar wind with the ordinary, not elevated solar wind density. The proton bulk speed is lower than 450 km/s and the proton density curve lies below the level of 10 particles per cm^3 . Therefore, the interval is ideal for the exploration of turbulence enhanced by products of magnetic reconnection at current sheets within and in the vicinity of the HPS.

5. IDENTIFICATION OF ELECTRON-DOMINATED CSS BY MEANS OF THE VELOCITY RATIO U_E/U_I

First, we create a list of ion CSs, following (Khabarova et al. 2021). At the next step we identify plasma structures presumably associated with electron-dominated CSs as predicted by the simulations discussed above. Such structures are supposed to be characterized by sharp variations in u_e/u_i and simultaneous variations in the IMF module B . Therefore, we identify them by calculating derivatives of u_e/u_i and

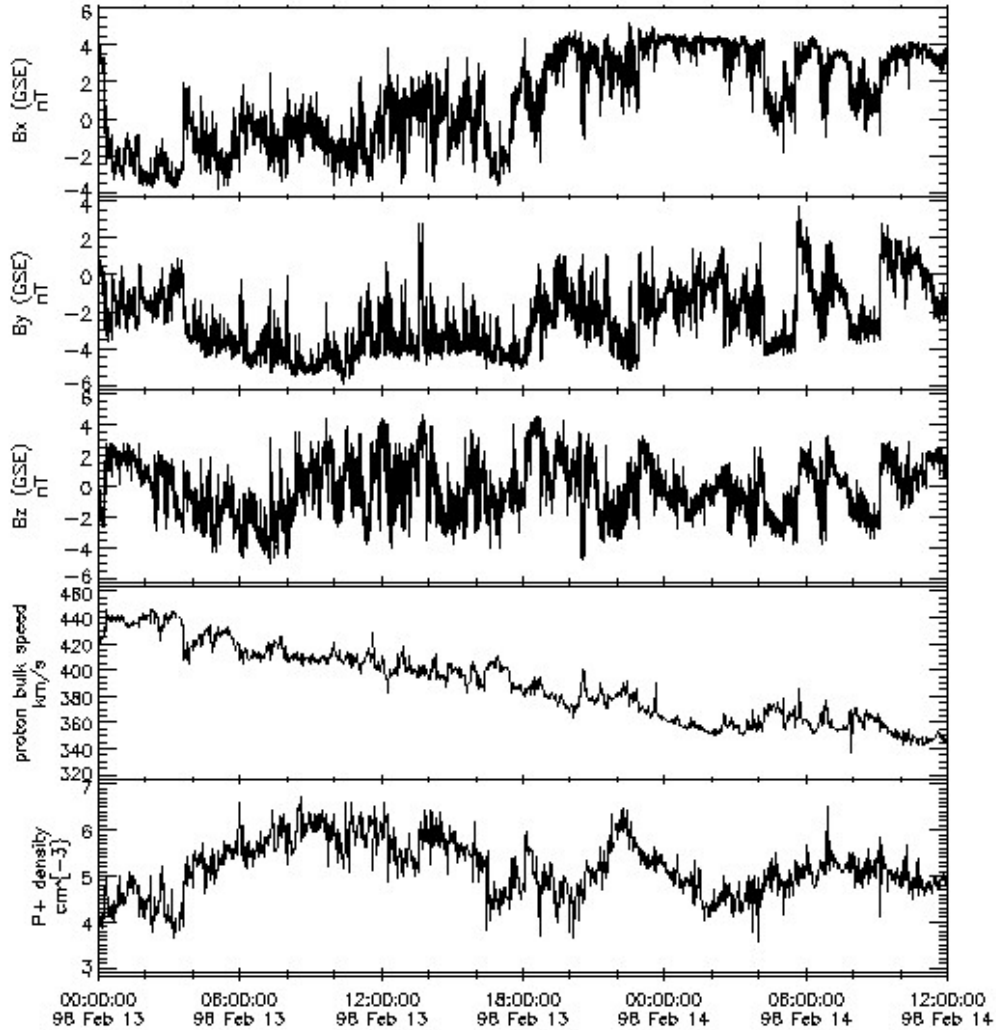


Figure 6. A period of a quiet solar wind: from 00:00 on February 13, 1998 to 12:00 on February 14, 1998. From top to bottom: the three components of the IMF in the GSE coordinate system, the proton bulk speed (u_i), and the proton density ($p+$) as observed by the Wind spacecraft.

B and setting up the noise thresholds as discussed below. Then we compare both rows to find similarities and differences.

Fig. 7 shows variations of the IMF strength in the upper panel, according to which one may approximately estimate how often and where the location of the strongest ion-determined CSs are crossed by the Wind spacecraft. Sharp dips in B seen with a one-second resolution correspond to crossings of neutral lines at CSs when at least one of the IMF components equals zero in the corresponding reference system. This is the simplest way to identify current sheets by eye known among observers. Additionally, β and Va/V variations are considered since statistics shows that the plasma beta jumps and the Va/V ratio falls at ion CSs. To make the changes more

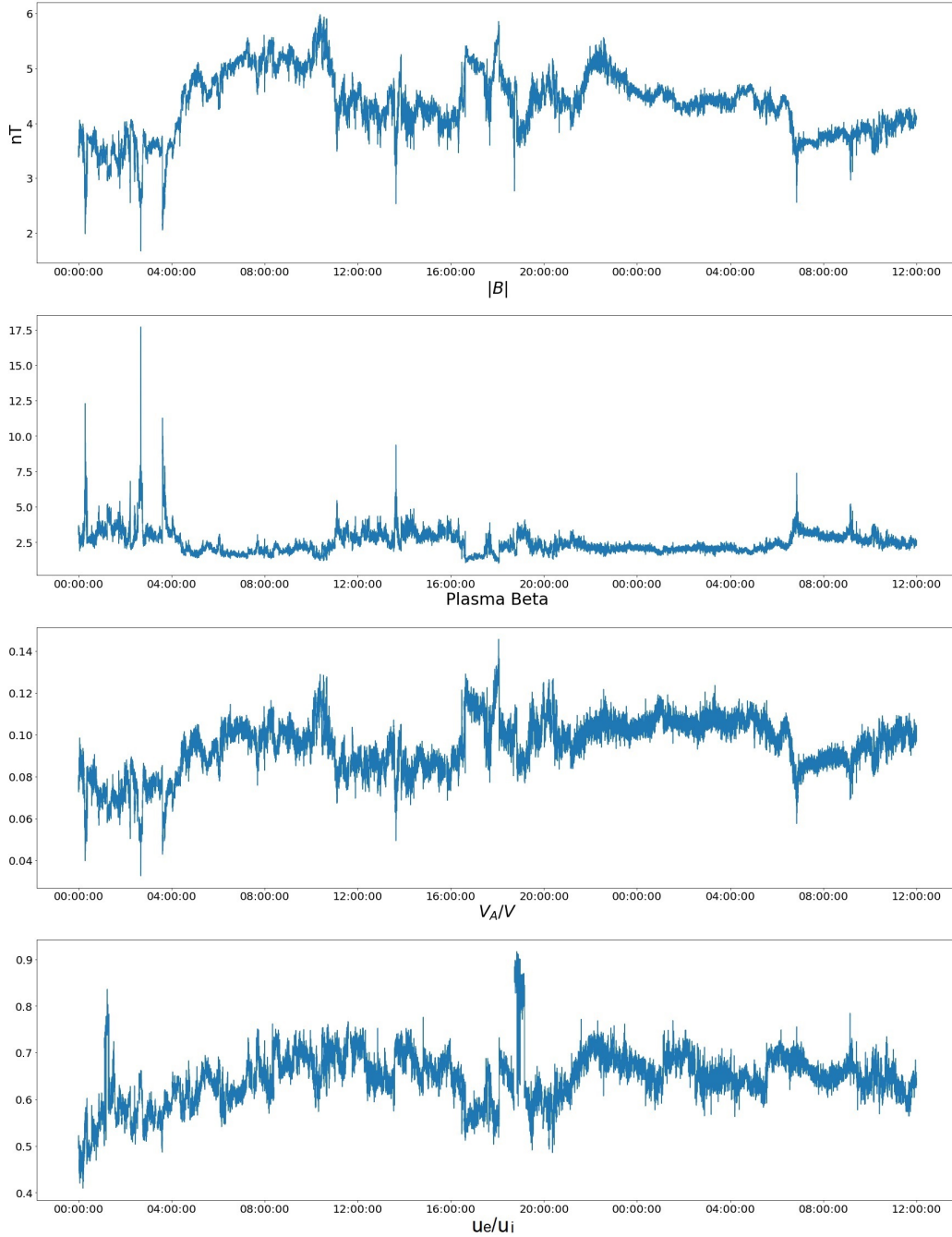


Figure 7. Key parameters helping identify both electron- and ion-dominated CSs for the same period as shown in Fig. 6. From top to bottom: the IMF strength B , β , V_A/V , and u_e/u_i .

pronounced, derivatives of these parameters are taken to identify CSs as described in (Khabarova et al. 2021).

It is important to explain why u_e/u_i is below 1 in the lower panel of Fig. 7 despite the fact that the theory predicts a u_e/u_i jump above 1 at electron-dominated CSs. The point is that this parameter is always below 1 in the background plasma around such

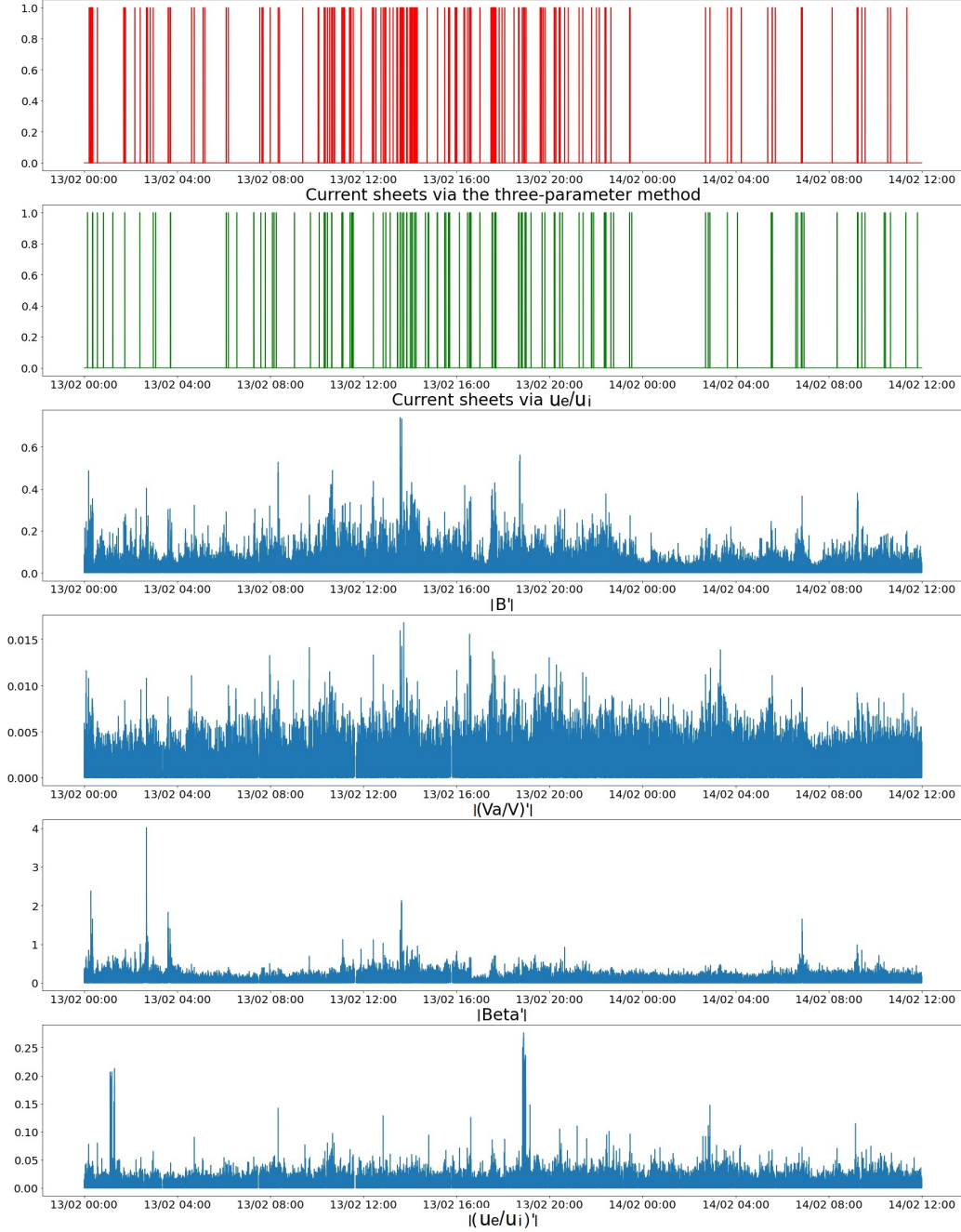


Figure 8. Location of ion- and electron-dominated CSs identified for the same period as shown in Fig. 6. From top to bottom: Location of ion-dominated CSs identified via the three-parameter method (Khabarova et al. 2021) (red lines) versus the location of electron-dominated CSs found via $(u_e/u_i)'$ and B' (green lines), respectively. Module of derivatives of B , V_A/V , β , and u_e/u_i used to show the sharpest changes in the parameters indicating CS crossings.

CSs. As we know from observations in the magnetosphere, CSs in which electrons carry the main electric current are mostly very thin, and a jump of the corresponding parameters at them can directly be seen with a high resolution only. However, the

available resolution of Wind measurements of u_e/u_i is 3 seconds, which means that the input of u_e/u_i sharp jumps above 1 into the 3-second-averaged picture is very low in the background of dominating u_e/u_i values far below 1. Only the strongest electron-dominated CSs can be detected with the 3-second resolution and seen as sharp increases of the u_e/u_i parameter in Fig. 7.

The result of the identification of ion CSs via the three-parameter method is shown in the first panel of Fig. 8 in the form of red bars. Zero means no CS and one corresponds to the presence of a CS identified with the application of the following thresholds that cut off the noise: $B' \leq -0.11$; $V_a/V \leq -0.005$; and $\beta \geq 0.75$. The other panels show variations in the parameters that help detect CSs with an automated method, running the corresponding code similar to that described in (Khabarova et al. 2021).

We have found that, analogous to the V_a/V parameter used in (Khabarova et al. 2021), u_e/u_i itself displays the location of current sheets worse than its derivative (compare the corresponding panels in Fig. 7 and Fig. 8). The second (green) panel in Fig. 8 shows the location of electron CSs identified using the proposed u_e/u_i parameter and B' . The corresponding noise-cutting threshold is $(u_e/u_i)' \geq 0.05$.

The other panels show variations in the parameters that help detect CSs with an automated method, running the corresponding code similar to that described in (Khabarova et al. 2021).

Although the exact location of ion CSs (red) and electron CSs (green) does not always coincide, the both red and green panels show clear clustering of CSs in the same places, and the strongest CS current sheets easily visible as the sharp B decreases and the plasma beta jumps are successfully identified via both $(u_e/u_i)'$ variations and the three-parameter method.

Some difference between the location of ion and electron current sheets can be explained, first, by the fact that the $(u_e/u_i)'$ parameter often catches an inner thin CS with the current produced by electrons, which is embedded in the wider "ion" current sheet. Purely technically, two methods having different accuracies always return a little different location of the corresponding structures. Second, the $(u_e/u_i)'$ parameter is supposed to be more sensitive to thin CSs born as a result of pure turbulence than to CSs produced by magnetic reconnection at strong large-scale CSs such as the HCS (see the Introduction).

Fig. 8 shows that despite very similar clustering, electron CSs may be observed without any association with ion CSs, and vice versa. This is an interesting result because this may reflect not just a different sensitivity of different methods but have a certain physical sense, allowing us to suggest that CSs of very different types can form under different conditions. However, a confirmation of this idea requires thorough investigations of properties of electron and ion CSs observed in the differently-originated solar wind flows or streams.

Therefore, preliminary results support the idea that the electron to proton velocity ratio can be considered as one of key parameters to detect electron-dominated CSs. Further studies will show details of how ion and electron-dominated CSs are related and why they sometimes exist separately.

6. CONCLUSIONS AND DISCUSSION

This study suggests a way to identify the strongest electron-dominated CSs in the solar wind despite a technical inability of most spacecraft ever operated in the heliosphere to resolve structures of electron-scales at which strong electron currents are supposed to flow.

Beginning with the first investigations of thin magnetospheric CSs based on the unique MMS data, it has been known that electrons carry the strongest electric current in CSs. Only electrons are significantly heated and move fast, while ions keep the average temperature and display no acceleration (Wang et al. 2018). Recent numerical simulations show that, indeed, electron-dominated CSs are associated with an increase of the electron-to-ion bulk speed ratio u_e/u_i and with electrons becoming the main carriers of the electric current.

Previous numerical studies of the CS formation in turbulent plasmas by fully kinetic as well as by hybrid code simulations (in which ions are considered as particles and electrons as a fluid) found that thin electron -scale CSs can be formed inside ion-scale thicker CSs (e.g., (Azizabadi et al. 2021; Malova et al. 2017)). Analytical modeling Simulations done for the magnetospheric conditions suggest show that electron-dominated CSs they can also exist independently of ion CSs (e.g., see (Zelenyi et al. 2020) and references therein).

High-accuracy observations of magneto-plasma structures at the magnetopause and in the tail of the terrestrial magnetosphere as well as in planetary magnetospheres show that electron current layers are usually found at sites where CSs become significantly thinned and ready for reconnection, or when magnetic reconnection is already underway (Nakamura et al. 2006; Panov et al. 2006; Runov et al. 2008; Grigorenko et al. 2019; Zelenyi et al. 2020; Hubbert et al. 2021). A thickness of such electron-dominated CSs may be as small as a few gyroradii of thermal electrons (Leonenko et al. 2021). Most of them are embedded in wider ion CSs, but single electron CSs can be observed too (Wang et al. 2018). Although Despite electron CSs possess very similar characteristics in different plasmas, their lifetime and stability are different (Zelenyi et al. 2008; Zelenyi et al. 2010; Zelenyi et al. 2019). It seems that pure pure electron CSs not associated with ion CSs are ubiquitous in the Martian magnetosphere but rather rare in the Earth's magnetotail.

So far, no pure electron CSs have been observed in the solar wind. The question regarding a typical width and stability of electron-dominated CSs in the solar wind still remains opened.

Beginning with the first studies of thin magnetospheric CSs based on the unique MMS data, it has been known that electrons carry the strongest electric current in electron CSs. Only electrons are significantly heated and move fast, while ions keep the average temperature and display no acceleration (Wang et al. 2018). Recent numerical simulations show that, indeed, electron-dominated CSs are associated with an increase of the electron-to-ion bulk speed ratio u_e/u_i and with electrons becoming the main carriers of the electric current.

Despite a growing understanding of physics of thin CSs in the magnetosphere, it is not clear the following question has remained opened: whether it is possible to find signatures of electron-dominated CSs in the solar wind plasma? Existing methods of identifying CSs in the heliosphere are focused on ion-dominated CSs, mainly considering the magnetic field behaviour and, rarely, the behaviour of plasma parameters (Khabarova et al. 2021).

Meanwhile, there are no comprehensive studies of electron-dominated scale CSs in the solar wind, for many technical reasons. Their automated identification and statistical investigations have been thought impossible for a long time. Even finding an approximate location of electron CSs is a difficult task, and case studies employing magnetospheric missions in the solar wind for this aim are extremely rare (e.g., (Mistry et al. 2015)). Meanwhile, Note that studying such CSs is especially important because simulations show that electron CSs most probably carry the largest electric currents in the solar wind (Podesta 2017).

To solve this problem at least partially herefore, we suggested to use indirect signatures of electron CSs based on the results of numerical simulations. In this study we applied the u_e/u_i criterion of the existence of an electron-dominated CS to the solar wind at 1 AU utilizing the Wind spacecraft data. We selected a quiet solar wind period within which numerous sharp variations of u_e/u_i were observed, suggesting that the most pronounced changes of $(u_e/u_i)'$ in a combination with those of B' may point out an approximate location of strong electron CSs, even analyzed at ion scales.

A confirmation came when the location of electron CSs identified that way was compared with the location of ion CSs identified via the other method (Khabarova et al. 2021). It was found that the structures presumably indicating electron-dominated CSs were mostly formed at/ or in the vicinity of ion-dominated CSs, showing the same clustering. An interesting point is that some of electron- and ion CSs were registered separately, without CSs of the other type found nearby.

Summarizing, we can report, for the first time, an important feature of CSs formed in the turbulent solar wind which is associated with electrons becoming the main current carriers. We conclude that the electron to proton velocity ratio may be considered as the major parameter identifying strong electron-dominated CSs and allowing an analysis of their properties in turbulent plasma. We suppose that only the strongest electron-dominated CSs can be identified in the solar wind via such a method. The reason for that is that the stronger the electric current carried by

electrons is, the higher the u_e/u_i parameter jumps. The higher it jumps over 1, the thinner the corresponding CS is (see Eq. 9). The thinner it is, the faster a spacecraft crosses such a structure, and, respectively, the larger an input of the surrounding low- u_e/u_i solar wind into the average value of u_e/u_i is. This effect smoothes the resulting picture of u_e/u_i variations, and only undoubtedly strong CSs with u_e/u_i exceeding 1 by far can be recognized in the solar wind with a one-three second resolution typical for most spacecraft.

The results testing the hypothesis of the importance of the u_e/u_i ratio in pointing to electron CSs are preliminary. Further studies are needed to find physical and statistical relation between the location and properties of ion and electron CSs. Here, we just report an important feature of the solar wind plasma which may be associated with thin CSs produced by electron currents. Electron CSs may be identified with a high degree of certainty only using several parameters, analogous to ion CSs, and with a high resolution. Future case studies employing data from the MMS mission will show what parameters are most important to find electron CS crossings and how to build a reliable method of electron CS identifying to investigate their properties statistically. So far, the proposed u_e/u_i method can be considered as potentially useful for studies of turbulence in the solar wind and probing CSs in space plasmas.

ACKNOWLEDGMENTS

The numerical simulations were supported by the German Science Foundation (DFG), project JA 2680-2-1. Part of the simulations were carried out on the HPC-Cluster of the Institute for Mathematics at the TU Berlin and the Max-Planck-Institute for Solar System Research Göttingen. The work is further supported by the German-Russian project DFG-RSF BU 777-16-1. The observational part of the study is supported and by the Russian Science Foundation grant No. 20-42-04418 (contributors: Olga Khabarova, Helmi Malova and Roman Kislov). We acknowledge using the following open-access data published via the NASA's SPDF website <https://cdaweb.gsfc.nasa.gov/index.html>: the magnetic field high-resolution definitive data (with many thanks to A. Koval, UMBC, NASA/GSFC) and the data on the velocity, the density, and the temperature of solar wind protons and electrons (with a gratitude to R. Lin and S. Bale, UC Berkeley) from the Wind spacecraft.

REFERENCES

- | | |
|---|--|
| <p>Azizabadi, A., Jain, N., & Büchner, J. 2021, <i>Phys. Plasmas</i>, 28, 052904, doi: 10.1063/5.0040692</p> <p>Bárta, M., Büchner, J., & Karlický, M. 2010, <i>Adv. Space Res.</i>, 45, 10, doi: 10.1016/j.asr.2009.07.025</p> | <p>Bárta, M., Büchner, J., Karlický, M., & Skála, J. 2011, <i>Astrophys. J.</i>, 737, 24, doi: 10.1088/0004-637X/737/1/24</p> <p>Biskamp, D., & Welter, H. 1989, <i>Phys. Fluids B</i>, 1, 1964</p> |
|---|--|

- Borovsky, J. E. 2010, *Phys. Rev. Lett.*, 105, 111102, doi: [10.1103/PhysRevLett.105.111102](https://doi.org/10.1103/PhysRevLett.105.111102)
- Borovsky, J. E., & Burkholder, B. L. 2020, *Journal of Geophysical Research: Space Physics*, 125, e2019JA027307, doi: [10.1029/2019JA027307](https://doi.org/10.1029/2019JA027307)
- Dahlin, J. T., Drake, J. F., & Swisdak, M. 2015, *Physics of Plasmas*, 22, 100704, doi: [10.1063/1.4933212](https://doi.org/10.1063/1.4933212)
- Daughton, W., Roytershteyn, V., Karimabadi, H., et al. 2011, *Nature Phys.*, 7, 539
- Dong, X. C., Dunlop, M. W., Wang, T. Y., et al. 2018, *Journal of Geophysical Research (Space Physics)*, 123, 5464, doi: [10.1029/2018JA025292](https://doi.org/10.1029/2018JA025292)
- Franci, L., Landi, S., Matteini, L., Verdini, A., & Hellinger, P. 2015, *Astrophys. J.*, 812, 21, doi: [10.1088/0004-637X/812/1/21](https://doi.org/10.1088/0004-637X/812/1/21)
- Greco, A., Matthaeus, W. H., Servidio, S., Chuychai, P., & Dmitruk, P. 2009, *Astrophys. J. Lett.*, 691, L111, doi: [10.1088/0004-637X/691/2/L111](https://doi.org/10.1088/0004-637X/691/2/L111)
- Grigorenko, E. E., Zelenyi, L. M., DiBraccio, G., et al. 2019, *J. Geophys. Res. Lett.*, 46, 6214, doi: [10.1029/2019GL082709](https://doi.org/10.1029/2019GL082709)
- Howes, G. G. 2016, *Astrophys. J. Lett.*, 827, L28. <http://stacks.iop.org/2041-8205/827/i=2/a=L28>
- Hubbert, M., Qi, Y., Russell, C. T., et al. 2021, *J. Geophys. Res. Lett.*, 48, e91364, doi: [10.1029/2020GL091364](https://doi.org/10.1029/2020GL091364)
- Jain, N., & Büchner, J. 2014a, *Phys. Plasmas*, 21, 062116, doi: [10.1063/1.4885636](https://doi.org/10.1063/1.4885636)
- . 2014b, *Phys. Plasmas*, 21, 072306, doi: [10.1063/1.4887279](https://doi.org/10.1063/1.4887279)
- Jain, N., Büchner, J., Comişel, H., & Motschmann, U. 2021, *Astrophys. J.*, 919, 103, doi: [10.3847/1538-4357/ac106c](https://doi.org/10.3847/1538-4357/ac106c)
- Kellogg, P. J., Bale, S. D., Mozer, F. S., Horbury, T. S., & Reme, H. 2006, *Astrophys. J.*, 645, 704, doi: [10.1086/499265](https://doi.org/10.1086/499265)
- Kellogg, P. J., Gurnett, D. A., Hospodarsky, G. B., et al. 2003, *Journal of Geophysical Research: Space Physics*, 108, doi: [10.1029/2002JA009312](https://doi.org/10.1029/2002JA009312)
- Khabarova, O., Sagitov, T., Kislov, R., & Li, G. 2021, *Journal of Geophysical Research: Space Physics*, 126, e2020JA029099, doi: [10.1029/2020JA029099](https://doi.org/10.1029/2020JA029099)
- Khabarova, O., Zank, G. P., Li, G., et al. 2015, *Astrophys. J.*, 808, 181, doi: [10.1088/0004-637X/808/2/181](https://doi.org/10.1088/0004-637X/808/2/181)
- Khabarova, O., Malandraki, O., Malova, H., et al. 2021, *Space Science Rev.*, 217, 38, doi: [10.1007/s11214-021-00814-x](https://doi.org/10.1007/s11214-021-00814-x)
- Khabarova, O. V., Zank, G. P., Li, G., et al. 2016, *Astrophys. J.*, 827, 122, doi: [10.3847/0004-637X/827/2/122](https://doi.org/10.3847/0004-637X/827/2/122)
- Lazarian, A., Eyink, G. L., Jafari, A., et al. 2020, *Physics of Plasmas*, 27, 012305, doi: [10.1063/1.5110603](https://doi.org/10.1063/1.5110603)
- Leonenko, M. V., Grigorenko, E. E., & Zelenyi, L. M. 2021, *Geomagnetism and Aeronomy*, 61, 688, doi: [10.1134/S0016793221050091](https://doi.org/10.1134/S0016793221050091)
- Li, G., Miao, B., Hu, Q., & Qin, G. 2011, *Phys. Rev. Lett.*, 106, 125001, doi: [10.1103/PhysRevLett.106.125001](https://doi.org/10.1103/PhysRevLett.106.125001)
- Maiewski, E. V., Malova, H. V., Kislov, R. A., et al. 2020, *Cosmic Research*, 58, 411, doi: [10.1134/S0010952520060076](https://doi.org/10.1134/S0010952520060076)
- Malova, H. V., Popov, V. Y., Delcourt, D. C., Petrukovich, A. A., & Zelenyi, L. M. 2013, *Journal of Geophysical Research (Space Physics)*, 118, 4308, doi: [10.1002/jgra.50390](https://doi.org/10.1002/jgra.50390)
- Malova, H. V., Popov, V. Y., Grigorenko, E. E., et al. 2017, *Astrophys. J.*, 834, 34, doi: [10.3847/1538-4357/834/1/34](https://doi.org/10.3847/1538-4357/834/1/34)
- Malova, H. V., Popov, V. Y., Mingalev, O. V., et al. 2012, *Journal of Geophysical Research (Space Physics)*, 117, A04212, doi: [10.1029/2011JA017359](https://doi.org/10.1029/2011JA017359)
- Maron, J., & Goldreich, P. 2001, *Astrophys. J.*, 554, 1175. <http://stacks.iop.org/0004-637X/554/i=2/a=1175>
- Matthaeus, W. H., Wan, M., Servidio, S., et al. 2015, *Phil. Trans. R. Soc. A*, 373, 20140154, doi: [10.1098/rsta.2014.0154](https://doi.org/10.1098/rsta.2014.0154)

- Mistry, R., Eastwood, J. P., Phan, T. D., & Hietala, H. 2015, *Geophysical Research Letters*, 42, 10,513, doi: <https://doi.org/10.1002/2015GL066820>
- Muñoz, P. A., & Büchner, J. 2018a, *Astrophys. J.*, 864, 92, doi: [10.3847/1538-4357/aad5e9](https://doi.org/10.3847/1538-4357/aad5e9)
- . 2018b, *Phys. Rev. E*, 98, 043205, doi: [10.1103/PhysRevE.98.043205](https://doi.org/10.1103/PhysRevE.98.043205)
- Muñoz, P. A., Kilian, P., & Büchner, J. 2014, *Phys. Plasmas*, 21, 112106, doi: [10.1063/1.4901033](https://doi.org/10.1063/1.4901033)
- Müller, J., Simon, S., Motschmann, U., et al. 2011, *Comput. Phys. Commun.*, 182, 946, doi: <http://dx.doi.org/10.1016/j.cpc.2010.12.033>
- Nakamura, R., Baumjohann, W., Asano, Y., et al. 2006, *Journal of Geophysical Research (Space Physics)*, 111, A11206, doi: [10.1029/2006JA011706](https://doi.org/10.1029/2006JA011706)
- Panov, E. V., Büchner, J., Fränz, M., et al. 2006, *Advances in Space Research*, 37, 1363, doi: [10.1016/j.asr.2005.08.024](https://doi.org/10.1016/j.asr.2005.08.024)
- Perri, S., Goldstein, M. L., Dorelli, J. C., & Sahraoui, F. 2012, *Phys. Rev. Lett.*, 109, 191101, doi: [10.1103/PhysRevLett.109.191101](https://doi.org/10.1103/PhysRevLett.109.191101)
- Petrukovich, A. A., Artemyev, A. V., Malova, H. V., et al. 2011, *Journal of Geophysical Research (Space Physics)*, 116, A00I25, doi: [10.1029/2010JA015749](https://doi.org/10.1029/2010JA015749)
- Pezzi, O., Pecora, F., Le Roux, J., et al. 2021, *Space Sci. Rev.*, 217, 39, doi: [10.1007/s11214-021-00799-7](https://doi.org/10.1007/s11214-021-00799-7)
- Phan, T. D., Eastwood, J. P., Cassak, P. A., et al. 2016, *J. Geophys. Res. Lett.*, 43, 6060, doi: [10.1002/2016GL069212](https://doi.org/10.1002/2016GL069212)
- Podesta, J. J. 2017, *J. Geophys. Res.: Space Phys.*, 122, 2795, doi: [10.1002/2016JA023629](https://doi.org/10.1002/2016JA023629)
- Podesta, J. J. 2017, *Solar Physics*, 292, 61, doi: [10.1007/s11207-017-1087-2](https://doi.org/10.1007/s11207-017-1087-2)
- Runov, A., Nakamura, R., Baumjohann, W., et al. 2003, *J. Geophys. Res. Lett.*, 30, 1579, doi: [10.1029/2002GL016730](https://doi.org/10.1029/2002GL016730)
- Runov, A., Sergeev, V. A., Nakamura, R., et al. 2006, *Annales Geophysicae*, 24, 247, doi: [10.5194/angeo-24-247-2006](https://doi.org/10.5194/angeo-24-247-2006)
- Runov, A., Baumjohann, W., Nakamura, R., et al. 2008, *Journal of Geophysical Research (Space Physics)*, 113, A07S27, doi: [10.1029/2007JA012685](https://doi.org/10.1029/2007JA012685)
- Sergeev, V. A., Mitchell, D. G., Russell, C. T., & Williams, D. J. 1993, *J. Geophys. Res.*, 98, 17345, doi: [10.1029/93JA01151](https://doi.org/10.1029/93JA01151)
- Sundkvist, D., Retinò, A., Vaivads, A., & Bale, S. D. 2007, *Phys. Rev. Lett.*, 99, 025004, doi: [10.1103/PhysRevLett.99.025004](https://doi.org/10.1103/PhysRevLett.99.025004)
- Syrovatskii, S. I. 1971, *Soviet Journal of Experimental and Theoretical Physics*, 33, 933
- Wang, R., Lu, Q., Nakamura, R., et al. 2018, *J. Geophys. Res. Lett.*, 45, 4542, doi: [10.1002/2017GL076330](https://doi.org/10.1002/2017GL076330)
- Zelenyi, L., Artemiev, A., Malova, H., & Popov, V. 2008, *Journal of Atmospheric and Solar-Terrestrial Physics*, 70, 325, doi: [10.1016/j.jastp.2007.08.019](https://doi.org/10.1016/j.jastp.2007.08.019)
- Zelenyi, L., Malova, H., Grigorenko, E., Popov, V., & Delcourt, D. 2019, *Plasma Physics and Controlled Fusion*, 61, 054002, doi: [10.1088/1361-6587/aafbbf](https://doi.org/10.1088/1361-6587/aafbbf)
- Zelenyi, L. M., Artemyev, A. V., Malova, K. V., Petrukovich, A. A., & Nakamura, R. 2010, *Phys. Usp.*, 53, 933, doi: [10.3367/UFNe.0180.201009g.0973](https://doi.org/10.3367/UFNe.0180.201009g.0973)
- Zelenyi, L. M., Malova, H. V., Artemyev, A. V., Popov, V. Y., & Petrukovich, A. A. 2011, *Plasma Physics Reports*, 37, 118, doi: [10.1134/S1063780X1102005X](https://doi.org/10.1134/S1063780X1102005X)
- Zelenyi, L. M., Malova, H. V., Grigorenko, E. E., Popov, V. Y., & Dubinin, E. M. 2020, *J. Geophys. Res. Lett.*, 47, e88422, doi: [10.1029/2020GL088422](https://doi.org/10.1029/2020GL088422)
- Zelenyi, L. M., Malova, H. V., Popov, V. Y., Delcourt, D., & Sharma, A. S. 2004, *Nonlinear Processes in Geophysics*, 11, 579, doi: [10.5194/npg-11-579-2004](https://doi.org/10.5194/npg-11-579-2004)